Polish J. Chem., **81**, 783–797 (2007)

Is the Aromaticity of the Benzene Ring in the $(\eta^6\text{-}C_6H_6)Cr(CO)_3$ Complex Larger than that of the Isolated Benzene Molecule?*

by F. Feixas[1], J.O.C. Jiménez-Halla[1], E. Matito[1,2], J. Poater[3] and M. Solà[1]**

[1]*Institut de Química Computacional and Departament de Química, Universitat de Girona, 17071 Girona, Catalonia, Spain*
e-mail: miquel.sola@udg.es
[2]*Institute of Physics, Szczecin University, 70-451 Szczecin, Poland*
[3]*Afdeling Theoretische Chemie, Scheikundig Laboratorium der Vrije Universiteit, De Boelelaan 1083, NL-1081 HV Amsterdam, The Netherlands*

(Received October 27th, 2006)

The aromaticity of the benzene ring in the $(\eta^6\text{-}C_6H_6)Cr(CO)_3$ complex is analyzed using several indicators of aromaticity based on different physical manifestations of this property. All indices used except NICS show that there is a clear reduction of the aromaticity of benzene upon coordination to the $Cr(CO)_3$ complex. The particular behavior of the NICS index has been analyzed in detail and we have concluded that the reduction of the NICS value in the benzene ring of the $(\eta^6\text{-}C_6H_6)Cr(CO)_3$ complex is not a manifestation of an increased aromaticity but is due to the ring currents generated by the electron pairs that take part in the benzene–$Cr(CO)_3$ bonding.

Key words: aromaticity, benzene, $(\eta^6\text{-}C_6H_6)Cr(CO)_3$ complex, Nucleus-Independent Chemical Shift (NICS), *Para*-Delocalization Index (PDI), Harmonic Oscillator Model of Aromaticity (HOMA), Aromatic Fluctuation Index (FLU), Six Center Index (SCI), Atoms in Molecules (AIM) Theory

$(\eta^6$-Arene)tricarbonylchromium complexes are among the most extensively studied half-sandwich complexes [1–6]. In the quest for new molecular switches, special attention has been focused on the reaction mechanisms of thermally induced inter-ring haptotropic rearrangements that occur in $(\eta^6$-arene)tricarbonylchromium complexes, in particular in those taking place in chromium tricarbonyl complexes of substituted naphthalenes [6–11], but also in larger polycyclic aromatic hydrocarbons (PAHs) [11–17]. The barrier to tripodal rotation of the $Cr(CO)_3$ fragment about the arene ring-Cr axis has also been the subject of many experimental and theoretical investigations [18–21].

Coordination of the chromium tricarbonyl complex to a given PAH takes place usually to the ring with the highest electron density [22,23], which is in many cases the most aromatic [24]. It is widely accepted that the structure, reactivity, and aroma-

* Dedicated to Professor T.M. Krygowski on the occasion of his 70th birthday.
**To whom correspondence should be addressed. E-mail: miquel.sola@udg.es
Phone: +34-972-418912. Fax: +34-972-418356.

ticity of the PAH are altered significantly upon complexation with the chromium tricarbonyl complex. Thus, after coordination the ring expands, loses its planarity, and shows an increased difference between alternated short and long C–C bonds [22,25]. Moreover, the reactivity of the coordinated ring dramatically changes due to complexation. The strong electron withdrawing character of the chromium tricarbonyl complex makes the coordinated PAH more susceptible to nucleophilic addition rather than electrophilic substitution and also increases the acidity of the aryl and benzylic hydrogens [25–27]. On the other hand, the effect of chromium tricarbonyl complexation on aromaticity is more controversial. According to Mitchell and coworkers [28–31], the benzene ring in tricarbonylchromium-complexed benzene is about 30–40% more aromatic than benzene itself. Their conclusion was based on chemical shift data and coupling constants which suggest that the benzene ring in certain annulene systems coordinated to the chromium tricarbonyl complex resists bond fixation better than the same ring in the uncomplexed annulene species does. Schleyer *et al.* [32] using nucleus-independent chemical shifts (NICS) and ^{1}H NMR chemical shifts data, concluded that the aromaticity of the benzene ring in $(\eta^{6}\text{-}C_6H_6)Cr(CO)_3$ is similar to that of the free benzene molecule. The authors found that NICS value computed in the centre of the benzene ring supports an increased aromatic character of the ring upon complexation, whereas the upfield ^{1}H NMR chemical shifts (and also ^{13}C NMR chemical shifts [9]) of the H atoms attached to the benzene ring by *ca*. 2 ppm and the positive value of the diamagnetic susceptibility exaltation point out the opposite conclusion [32]. In fact, Simion and Sorensen [33] ten years before concluded from diamagnetic susceptibility exaltation data that the benzene ring coordinated to the chromium tricarbonyl complex is antiaromatic. A similar opinion is hold by Hubig *et al.* [25] who consider that the charge transfer from the arene to the transition metal in metal-arene coordination leads to a complete loss of the aromaticity of the π-system.

In this context, the aim of the present paper is to shed light on the controversial aromaticity of the benzene ring coordinated to the chromium tricarbonyl complex, a question that has been debated for about 40 years [34]. The evaluation of aromaticity is usually performed by analyzing its manifestations and this leads to the classical structural, magnetic, energetic, and reactivity-based measures of aromaticity [35,36]. At this point, we must note the important contribution by Katritzky-Krygowski and co-workers who found, by means of principal component analyses, that aromaticity is a multidimensional property and, as a consequence, aromatic compounds are better characterized using a set of indexes based on different physical properties [36–40]. Most aromaticity studies of PAHs coordinated to $Cr(CO)_3$ have employed a single magnetic descriptor of aromaticity or a set of magnetic-based indices. Here we propose to use a set of indices that take into account structural, electronic, and magnetic manifestations of aromaticity.

Descriptors of aromaticity. As a structure-based measure, we have made use of the harmonic oscillator model of aromaticity (HOMA) index, defined in a landmark study by Kruszewski and Krygowski [41,42] as:

$$HOMA = 1 - \frac{\alpha}{n}\sum_{i=1}^{n}(R_{opt} - R_i)^2 \quad (1)$$

where n is the number of bonds considered, and α is an empirical constant (for C–C bonds α = 257.7) fixed to give HOMA = 0 for a model nonaromatic system, and HOMA = 1 for a system with all bonds equal to an optimal value R_{opt} (1.388 Å for C–C bonds), assumed to be achieved for fully aromatic systems. R_i stands for a running bond length. This index has been found to be one of the most effective structural indicators of aromaticity [39,43].

Magnetic indices of aromaticity are based on the π-electron ring current that is induced when the system is exposed to external magnetic fields. In this work, we have used the NICS, proposed by Schleyer and co-workers [44–46], as a magnetic descriptor of aromaticity. It is defined as the negative value of the absolute shielding computed at a ring centre or at some other interesting point of the system. Rings with large negative NICS values are considered aromatic.

Three aromaticity criteria based on electron delocalization have been employed [47]. These indexes try to measure the cyclic electron delocalization of mobile electrons in aromatic rings. First, the *para*-delocalization index (PDI) [48,49], which is obtained using the delocalization index (DI) [50,51] as defined in the framework of the Atoms in Molecules (AIM) theory of Bader [52–54]. The PDI is an average of all DI of *para*-related carbon atoms in a given six-membered ring. The DI value between atoms A and B, δ(A,B), is obtained by double integration of the exchange-correlation density $\Gamma_{XC}(\vec{\mathbf{r}}_1, \vec{\mathbf{r}}_2)$ over the basins of atoms A and B, which are defined from the condition of zero-flux gradient in the one-electron density, $\rho(\mathbf{r})$ [52–54]:

$$\delta(A,B) = -2\int_A\int_B \Gamma_{XC}(\vec{\mathbf{r}}_1, \vec{\mathbf{r}}_2)d\vec{\mathbf{r}}_1 d\vec{\mathbf{r}}_2 \quad (2)$$

For closed-shell monodeterminantal wavefunctions one obtains:

$$\delta(A,B) = 4\sum_{i,j}^{N/2} S_{ij}(A)S_{ij}(B) \quad (3)$$

The summations in Eq. (3) run over all the N/2 occupied molecular orbitals. S_{ij}(A) is the overlap of the molecular orbitals i and j within the basin of atom A. δ(A,B) provides a quantitative idea of the number of electron pairs delocalized or shared between atoms A and B. Previous works [48,49,55,56] have shown that for a series of planar and curved polycyclic aromatic hydrocarbons there is a satisfactory correlation between NICS, HOMA, and PDI.

As the second index based on electronic delocalization, we have used the aromatic fluctuation index (FLU) [57], which describes the fluctuation of electronic

charge between adjacent atoms in a given ring. The FLU index is based on the fact that aromaticity is related to the cyclic delocalized circulation of π electrons, and it is constructed by considering the amount of electron sharing between contiguous atoms, which should be substantial in aromatic molecules, and also by taking into account the similarity of electron sharing between adjacent atoms. It is defined as:

$$FLU = \frac{1}{n} \sum_{A-B}^{RING} \left[\left(\frac{V(B)}{V(A)} \right)^{\alpha} \left(\frac{\delta(A,B) - \delta_{ref}(A,B)}{\delta_{ref}(A,B)} \right) \right]^2 \tag{4}$$

with the sum running over all adjacent pairs of atoms around the ring, n being equal to the number of members in the ring, $\delta_{ref}(C,C) = 1.4$ (the $\delta(C,C)$ value in benzene at the HF/6-31G(d) level [57]), and $V(A)$ is the global delocalization of atom A given by:

$$V(A) = \sum_{B \neq A} \delta(A,B) \tag{5}$$

Finally, α is a simple function to make sure that the first term in Eq. (4) is always greater or equal to 1, so it takes the values:

$$\alpha = \begin{cases} 1 & V(B) > V(A) \\ -1 & V(B) \leq V(A) \end{cases} \tag{6}$$

Third, the Six Center Index (SCI), which is a class of multicenter index that provides another good measure of aromaticity [58,59]. For closed-shell monodeterminantal wavefunctions it reads:

$$SCI = \frac{16}{3} \sum_{\alpha} \sum_{i,j,k,l,m,n}^{N/2} \Gamma_{\alpha} [S_{ij}(A) S_{jk}(B) S_{kl}(C) S_{lm}(D) S_{mn}(E) S_{ni}(F)] \tag{7}$$

where Γ_α stands for a permutation operator which interchanges the atomic labels A, B, ..., F to generate up to 6! combinations. For the indexes used, we have that the more negative the NICS, the lower the FLU index, and the higher the HOMA, PDI, and SCI values, the more aromatic the rings are.

Computational details. All calculations have been performed with the Gaussian 03 [60] and AIMPAC [61] packages of programs, at the B3LYP level of theory [62–64] with the 6-31G(d,p) basis set [65–67]. All aromaticity criteria have also been evaluated at the same B3LYP/6-31G(d,p) level of theory.

The GIAO method [68] has been used to perform calculations of NICS at ring centres (NICS(0)) determined by the non-weighted mean of the heavy atoms coordinates and at several distances above and below the centre of the ring taken into analysis.

Calculation of atomic overlap matrices and computation of DI and SCI were performed with the AIMPAC [61] and ESI-3D [69] collection of programs. Calculation of these DIs with the density functional theory (DFT) cannot be performed exactly because the electron-pair density is not available at this level of theory [70]. As an approximation, we have used the Kohn-Sham orbitals obtained from a DFT calculation to compute Hartree-Fock-like DIs through Eq. (3), which does not account for electron correlation effects. In practice the values of the DIs obtained using this approximation are generally closer to the Hartree-Fock values than correlated DIs obtained with a configuration interaction method [70,71]. The numerical accuracy of the AIM calculations has been assessed using two criteria: i) The integration of the Laplacian of the electron density ($\nabla^2\rho(r)$) within an atomic basin must be close to zero; ii) The number of electrons in a molecule must be equal to the sum of all the electron populations of the molecule, and also equal to the sum of all the localization indices and half of the delocalization indices in the molecule. For all atomic calculations, integrated absolute values of $\nabla^2\rho(r)$ were always less than 0.001 a.u. For all molecules, errors in the calculated number of electrons were always less than 0.01 a.u.

RESULTS AND DISCUSSION

The B3LYP/6-31G(d,p) optimization of benzene leads to a C–C bond length of 1.397 Å not far from the experimental [72] and CCSD/TZ2P [73] results of 1.390 and 1.392 Å, respectively. The B3LYP/6-31G(d,p) optimized structure of $(\eta^6\text{-}C_6H_6)Cr(CO)_3$ in Figure 1 is also very close to that obtained experimentally by X-ray and neutron diffraction [74,75] and to that reported by previous theoretical calculations [19,32,76]. In the experimental and theoretical molecular structure, the $Cr(CO)_3$ group is placed staggered with respect to the C–H bonds of benzene to reduce steric repulsions. The average C–C bond length in benzene when coordinated to $Cr(CO)_3$ is 1.415 Å. Therefore, after coordination there is an expansion of the benzene ring corresponding to an average increase of the C–C bond length of 0.018 Å. Coordination also induces a bond length alternation (BLA) between short and long C–C bonds of 0.019 Å. The B3LYP/6-31G(d,p) distance from the Cr atom to the center of the ring is 1.720 Å (exp.: 1.724–1.726 Å) [74,75]. Interestingly, there is a significant pyramidalization of the C atoms measured from the ∠CCCH dihedral angle of about 178° that leads to a benzyl hydrogen atoms slightly bent towards the $Cr(CO)_3$ fragment [19]. In particular, the H atoms are 0.033 Å (exp.: 0.03 Å [75]) displaced from the plane defined by the C atoms of the benzene ring. The calculated B3LYP/6-31G(d,p) binding energy of benzene in $(\eta^6\text{-}C_6H_6)Cr(CO)_3$ is 67.0 kcal·mol^{-1}, a value significantly larger than the experimental result of 53 kcal·mol^{-1} [77]. We attribute the difference, in part, to the lack of basis set superposition error correction in our calculations, which is expected to reduce the computed binding energy by at least 7 kcal·mol^{-1} as inferred from the calculations of Furet and Weber [76] using a similar basis set.

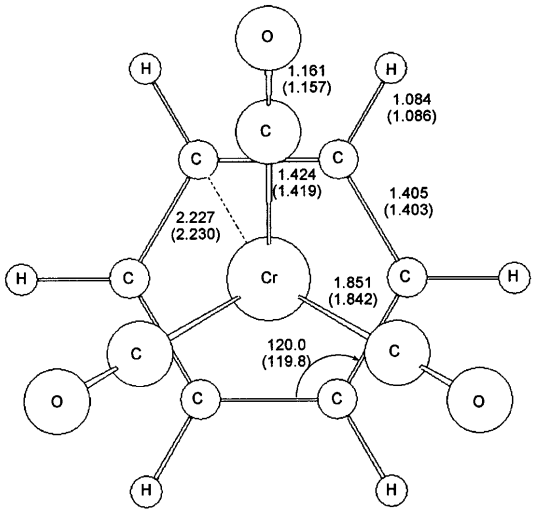

Figure 1. Most relevant optimized B3LYP/6-31G(d,p) and experimental [75] (in parentheses) bond lengths and angles of the $(\eta^6\text{-}C_6H_6)Cr(CO)_3$ complex. Distances in Å and angles in degrees.

The nature of the bond between the arene and the metal in (η^6-arene)tricarbonylchromium complexes was discussed by Albright, Hoffmann, and coworkers some years ago [78]. These authors found that the interaction of the degenerate *2e* LUMO and $2a_1$ LUMO+1 orbitals with the highest occupied π-orbitals of the arene with the appropriated symmetry is the dominant bonding mechanism [22]. Charge transfer from the highest occupied π-orbitals of the arene to the lowest unoccupied *2e* and $2a_1$ orbitals of $Cr(CO)_3$ partially breaks the C–C bonds, thus explaining the observed expansion of the aromatic ring and the increase in BLA in $(\eta^6\text{-}C_6H_6)Cr(CO)_3$. The pyramidalization of the C atoms in the ring moves somewhat the π-electron density to the center of the benzene ring, thus favoring the interaction between the highest occupied π-orbitals of benzene and the unoccupied *2e* and $2a_1$ orbitals of $Cr(CO)_3$. The bonding mechanism in (η^6-arene)tricarbonylchromium complexes indicates that donation is larger than backdonation (as in carbenes [79]) and, as a consequence, the electron-rich arene is transformed into an electron-poor acceptor and a target for nucleophilic attacks [22]. The charge transfer from the benzene ring to the $Cr(CO)_3$ fragment in the optimized $(\eta^6\text{-}C_6H_6)Cr(CO)_3$ complex is 0.866 e (see Table 1) according to the generalized atomic polar tensor (GAPT) charges defined by Cioslowski [80].

Because of the loss of π electron density in the ring, one should expect a partially disruption of aromaticity in the benzene ring of $(\eta^6\text{-}C_6H_6)Cr(CO)_3$ in comparison to free benzene, as discussed by Hubig *et al*. [25]. This is also something expected from the BLA and bond length elongation that the benzene ring experiences upon coordination [81,82]. Indeed, this is what most indicators of aromaticity used in the present work show. The HOMA of the benzene ring changes from 0.981 to 0.796 when going

from free to coordinated benzene. PDI and SCI also decrease in the same direction from 0.103 to 0.036 e and from 0.075 to 0.019 e, respectively. Finally, the FLU index slightly increases from 0.000 in isolated benzene to 0.009 in the benzene ring of the $(\eta^6\text{-}C_6H_6)Cr(CO)_3$ complex. Thus, HOMA, PDI, FLU, and SCI indexes indicate the expected reduction of the aromaticity of the benzene ring upon complexation. Moreover, PDI, FLU, and SCI values in Table 1 show a steady reduction of aromaticity when the distance between the Cr atom and the benzene ring is reduced.

Table 1. PDI (electrons), FLU, SCI (electrons), and GAPT charge on the benzene ring (electrons) for the complex at different $Cr–C_6H_6$ distances (in Å)[a,b].

$R(Cr–C_6H_6)$[c]	PDI	FLU	SCI	GAPT charge
1.22	0.019	0.019	0.009	1.035
1.42	0.022	0.014	0.012	0.997
1.62	0.031	0.010	0.017	0.917
1.72	0.036	0.009	0.019	0.866
1.82	0.044	0.007	0.024	0.812
2.02	0.059	0.005	0.033	0.699
2.22	0.073	0.003	0.042	0.579
2.42	0.085	0.002	0.051	0.451
2.62	0.093	0.001	0.059	0.321
2.82	0.097	0.001	0.064	0.207
3.02	0.101	0.001	0.067	0.124
3.22	0.102	0.001	0.070	0.073
3.42	0.103	0.000	0.071	0.040
3.62	0.103	0.000	0.073	0.025
3.82	0.103	0.000	0.073	0.017
4.02	0.103	0.000	0.074	0.012
4.22	0.103	0.000	0.074	0.011
4.42	0.103	0.000	0.074	0.011
4.62	0.103	0.000	0.075	0.009

[a]For comparison, the PDI, FLU, and SCI values for the free benzene are 0.103 e, 0.000, and 0.075 e at the B3LYP/6-31G(d,p) level of theory.
[b]Only the $R(Cr–C_6H_6)$ is changed at each point. The rest of structural parameters are frozen to the values that they have in the B3LYP/6-31G(d,p) optimized structure of the $(\eta^6\text{-}C_6H_6)Cr(CO)_3$ complex.
[c]The B3LYP/6-31G(d,p) optimized structure (see Figure 1) corresponds to $R(Cr–C_6H_6)$ = 1.72 Å.

As reported by Schleyer and coworkers [46], we find that the magnetic-based NICS(0) index of benzene complexed to $Cr(CO)_3$ is much larger in absolute value than the NICS(0) of free benzene (–26.7 *vs*. –9.9 ppm), thus indicating an increase of

aromaticity when benzene is coordinated to $Cr(CO)_3$, as claimed by Mitchell and coworkers [28–31]. Using NICS(1) similar results are obtained. We have also analyzed the out-of-plane component of the NICS(0), the $NICS(0)_{zz}$, which is considered to be a better NICS-based indicator of aromaticity [83,84]. In this case, we recover the expected result of a clear reduction of aromaticity when going from benzene ($NICS(0)_{zz}$ = –14.3 ppm) to the $(\eta^6\text{-}C_6H_6)Cr(CO)_3$ complex ($NICS(0)_{zz}$ = –7.4 ppm). Thus, all analyzed indexes (including $NICS_{zz}$ and $NICS_\pi$ [46]) except NICS denote neither an increase of aromaticity [28–31] nor a constant aromaticity [32] but a clear decrease of the aromaticity of the benzene ring upon coordination. This result is not surprising if one takes into account the bonding mechanism of benzene to the $Cr(CO)_3$ complex discussed above.

At this stage the reason for the breakdown of NICS in this particular species is unclear. In previous works [85,86], some of us showed that the failure of NICS to measure local aromaticity in π-stacked species is due to the coupling between magnetic fields coming from aromatic rings located above or below the analyzed ring. With this in mind, a possible hypothesis that may explain the breakdown of NICS to show a reduction of aromaticity of the benzene ring upon complexation is that the observed NICS reduction in the $(\eta^6\text{-}C_6H_6)Cr(CO)_3$ complex does not correspond to a real aromaticity increase of the benzene ring but to the couplings between the induced magnetic fields of the $Cr(CO)_3$ and benzene fragments. To check this hypothesis, we have summed the NICS profiles of the ground state of the optimized and isolated $Cr(CO)_3$ and benzene species (see Figure 2) placing the benzene and $Cr(CO)_3$ complex at the same ring–metal distance as that of the optimized $(\eta^6\text{-}C_6H_6)Cr(CO)_3$ complex without further reoptimization of the two fragments. The NICS profile obtained together with that of the $(\eta^6\text{-}C_6H_6)Cr(CO)_3$ complex are shown in Figure 3a. As can be seen, the NICS(0) of the optimized $(\eta^6\text{-}C_6H_6)Cr(CO)_3$ complex is much more negative than that corresponding to the sum of the C_6H_6 and $Cr(CO)_3$ profiles. The latter sum of profiles simulates the NICS profile that results from the direct coupling of the induced magnetic fields generated by the unperturbed densities of the isolated C_6H_6 and $Cr(CO)_3$ fragments brought together at the $R(Cr–C_6H_6)$ = 1.720 Å distance. This means that there is a remarkable change of the NICS profile upon complexation that must be attributed to the formation of the chemical bond between benzene and $Cr(CO)_3$ in the $(\eta^6\text{-}C_6H_6)Cr(CO)_3$ complex. So, the observed change in NICS profile has to be mainly produced by the magnetic field generated by the electron pairs that participate most in the formation of the chemical bond between C_6H_6 and the metal. These electron pairs become more delocalized after bond formation and can contribute more to the total ring current and the induced magnetic field at a given point. This hypothesis is confirmed by the profiles that are obtained by increasing the $R(Cr–C_6H_6)$ with increments of 0.5 Å without reoptimization of the complex and the fragments. As can be seen in Figure 3, for a $R(Cr–C_6H_6)$ = 3.220 Å (and also for larger distances) the NICS profile of the $(\eta^6\text{-}C_6H_6)Cr(CO)_3$ complex and that corresponding to the sum of the isolated C_6H_6 and $Cr(CO)_3$ fragments are almost the same. This is so, because at this distance the chemical bond is not formed. Indeed, the charge

transfer according to GAPT charges is only 0.07 e, so the interaction between the two fragments is residual. The small differences found in the two profiles at R(Cr–C_6H_6) = 3.220 Å are basically due to the different geometries of the C_6H_6 system. For the NICS profile of the (η^6-C_6H_6)$Cr(CO)_3$ complex, we took the geometry of the C_6H_6 in the complex which differs from the equilibrium geometry because, as said before, the ring expands and undergoes BLA upon complexation. Because of the geometry differences, the NICS profile of the deformed benzene differs from that of the isolated benzene molecule, the former showing as expected a somewhat smaller aromatic character.

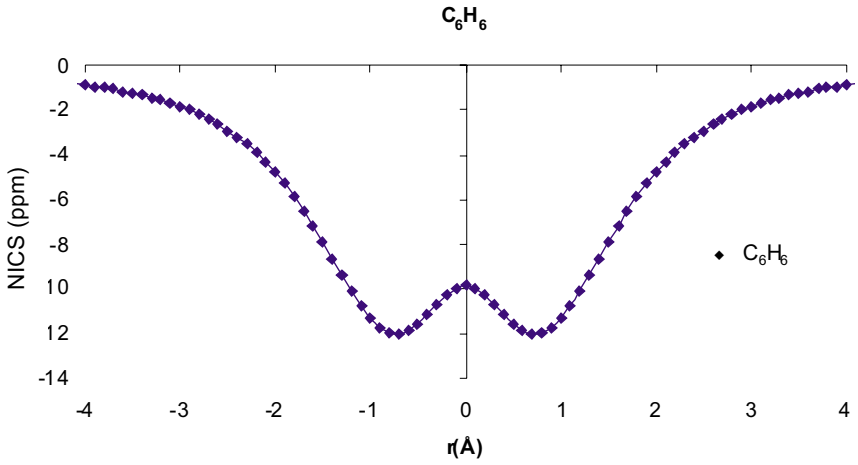

(a)

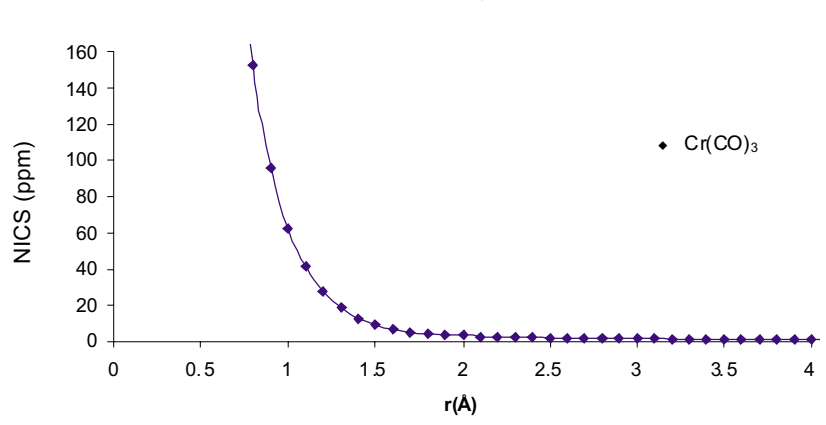

(b)

Figure 2. B3LYP/6-31G(d,p) NICS profiles (in ppm) of the isolated and optimized (a) benzene and (b) $Cr(CO)_3$ complex. The benzene profile starts at the ring centre and moves in the direction perpendicular to the plane defined by the ring. The $Cr(CO)_3$ profile starts at the Cr atom and moves in the direction away from the $Cr(CO)_3$ complex along the C_3 axis.

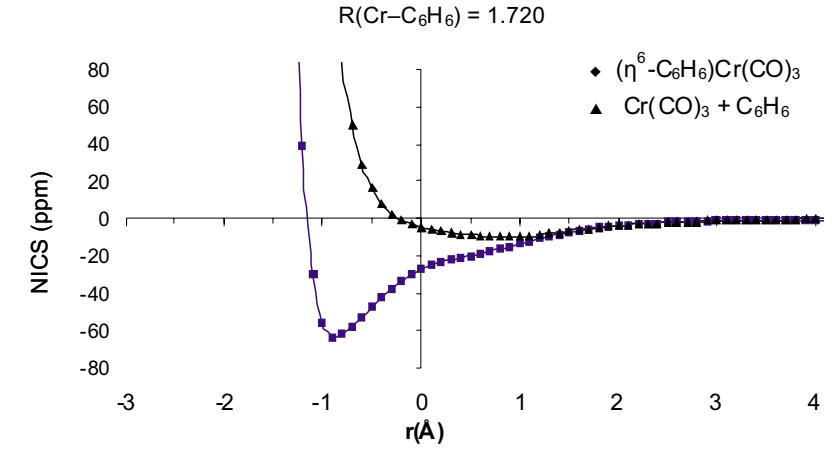

(a)

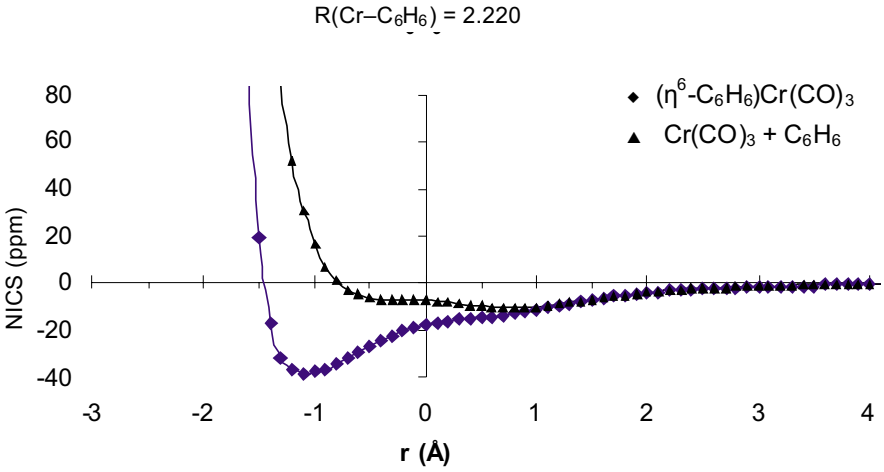

(b)

Figure 3. Comparison between the B3LYP/6-31G(d,p) NICS profiles (in ppm) of the $(\eta^6\text{-}C_6H_6)Cr(CO)_3$ complex and the sum of the NICS profiles of the isolated and optimized benzene and $Cr(CO)_3$ complex for different $Cr–C_6H_6$ distances (in Å). Positive (negative) **r** values correspond to points located in the C_3 axis at a distance **r** from the ring centre away from (towards) the $Cr(CO)_3$ complex.

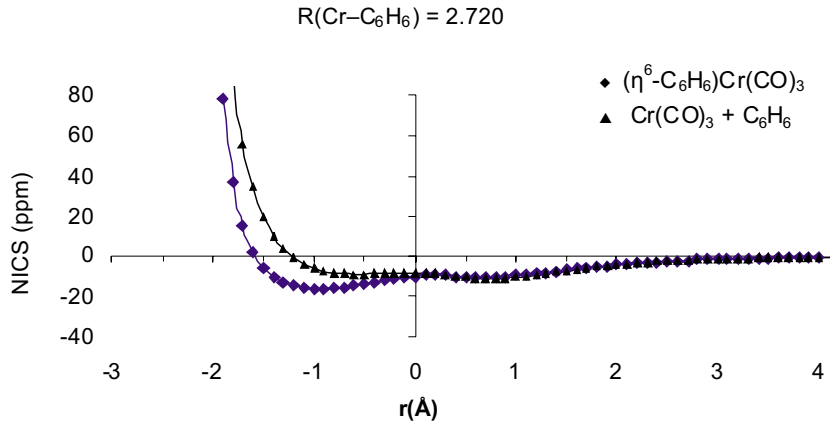

(c)

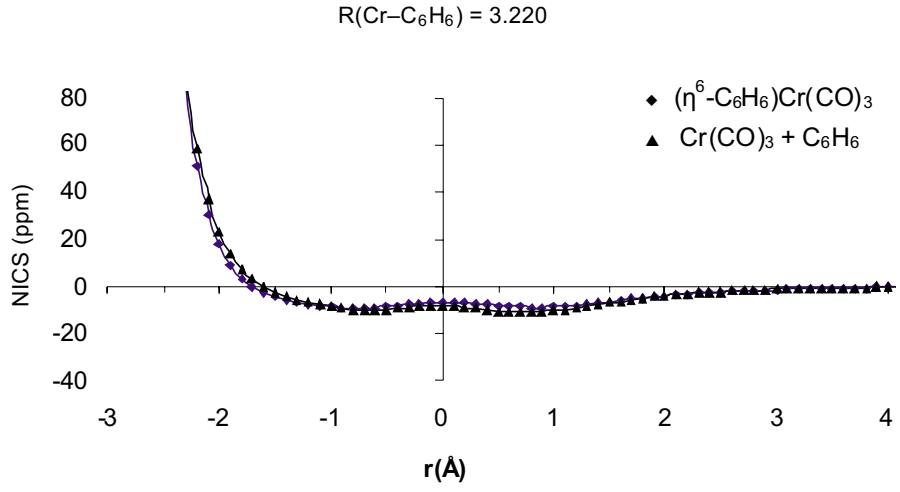

(d)

Figure 3. Continuation

Finally, we have represented in Figure 4, the NICS surface obtained by changing both the R(Cr–C_6H_6) distance and the distance **r** from the center of the ring to a given point located at the C_3 axis of the (η^6-C_6H_6)$Cr(CO)_3$ complex, using for benzene and $Cr(CO)_3$ the same geometries as those of the equilibrium structure of the complex. The horizontal lines shown in Figure 4 generate NICS(0), NICS(1), and NICS(-1) profiles for different R(Cr–C_6H_6) distances. As can be seen in Figure 4, both NICS(0) and NICS(-1) decrease steadily when going from long to short R(Cr–C_6H_6) distances starting from *ca*. 4 Å, thus indicating an increased aromaticity character of the ring

which, as shown before, is not real but due to bond formation. The vertical dashed line provides a NICS profile, as those depicted in Figure 3, for a given R(Cr–C_6H_6) distance (in the particular case of Figure 4, R(Cr–C_6H_6) = 1.720 Å). It is noteworthy that for R(Cr–C_6H_6) distances of about 3 Å (small vertical solid line in Figure 4) or larger, one gets NICS profiles with a clear double-well profile similar to that found for the isolated benzene molecule (see Figure 2a) with a local maximum of NICS at the ring center and minima located slightly above and below 1 Å from the ring center in the direction perpendicular to the molecular plane. For large R(Cr–C_6H_6)

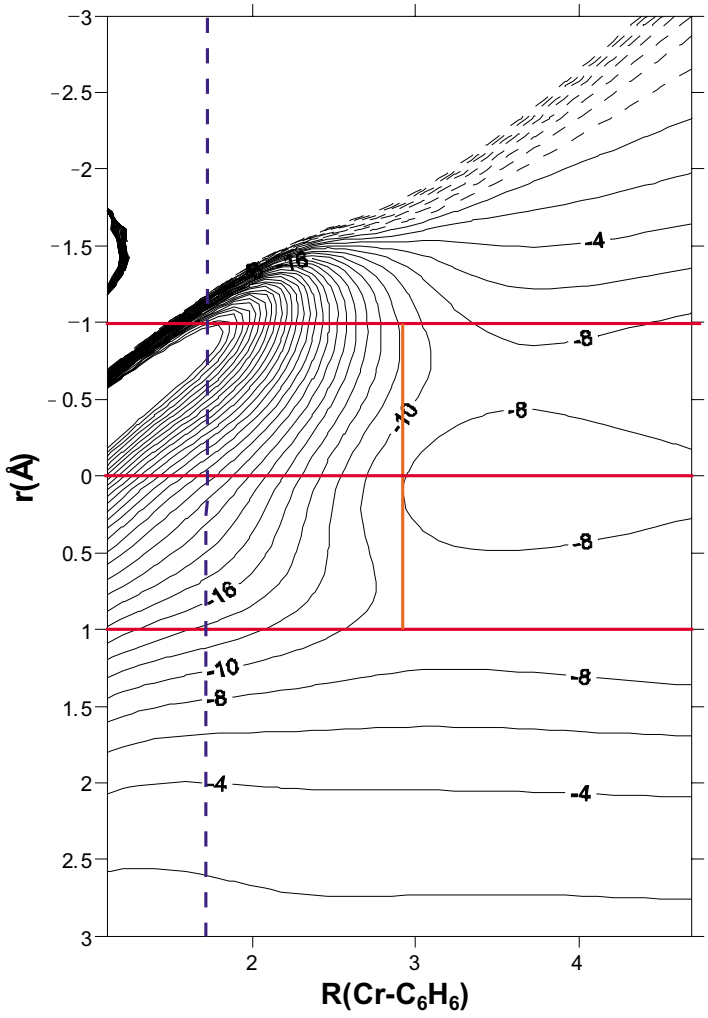

Figure 4. B3LYP/6-31G(d,p) NICS surface (in ppm) of the (η^6-C_6H_6)$Cr(CO)_3$complex. Positive (negative) **r** values correspond to points located in the C_3 axis at a distance **r** from the ring centre away from (towards) the $Cr(CO)_3$ complex. The geometry of the (η^6-C_6H_6)$Cr(CO)_3$ complex is kept unchanged and only the Cr–C_6H_6 distances are varied from approximately 1 to 5 Å.

distances, the bond between benzene and the $Cr(CO)_3$ group is not formed and thus the NICS profiles of the $(\eta^6\text{-}C_6H_6)Cr(CO)_3$ complex keep almost invariant.

CONCLUSIONS

In this work, we have analyzed the controversial aromaticity of the benzene ring coordinated to the $Cr(CO)_3$ complex. We have shown that a geometric descriptor like HOMA, a magnetic index like $NICS_{zz}$, and several electronic measures of aromaticity such as PDI, FLU, and SCI, indicate that there is a clear reduction of aromaticity of the benzene ring upon complexation as expected from the bonding mechanism. In our opinion, the result obtained with these five indexes is clear and should end the debate about the aromaticity of the benzene ring in the $(\eta^6\text{-}C_6H_6)Cr(CO)_3$ complex. Somewhat surprisingly, the NICS index erroneously denotes a larger aromaticity of the benzene ring in the $(\eta^6\text{-}C_6H_6)Cr(CO)_3$ complex than in benzene itself. We have analyzed the reason for this failure of the NICS index and we have concluded that the extra delocalization gained by the electron pairs that contribute the most to the chemical bond explains the reduction of the NICS value. Therefore, the NICS reduction is not the result of a larger aromaticity but the result of increased ring currents due to bond formation. This result suggests exercising caution in the use of single-point NICS or NICS scans as a quantitative measure of aromaticity for aromatic rings in transition metal complexes. Finally, it is worth noting that $NICS_{zz}$ is a more reliable index of aromaticity for this particular system.

Acknowledgments

Financial help has been furnished by the Spanish Ministerio de Educación y Ciencia (MEC) project No. CTQ2005-08797-C02-01/BQU and by the Catalan Departament d'Universitats, Recerca i Societat de la Informació (DURSI) of the Generalitat de Catalunya project No. 2005SGR-00238. F.F. and E.M. thank the MEC for the doctoral fellowships no. AP2005-2997 and AP2002-0581, respectively. JOCJH thanks the DURSI for financial support through the grant 2005FI/00451. J.P. also acknowledges the European Union for a Marie Curie fellowship. We also thank the Centre de Supercomputació de Catalunya (CESCA) for partial funding of computer time.

Dedication

This work is dedicated to Prof. Tadeusz Marek Krygowski as a proof of our admiration for his brilliant contributions to chemistry.

REFERENCES

1. Mann B.E., *Chem. Soc. Rev.*, **15**, 167 (1986).
2. Dötz K.H. and Stendel J., Jr., Modern Arene Chemistry, Astruc D. (ed), Wiley-VCH, Weinheim, p. 250 (2002).
3. Dötz K.H., Szesni N., Nieger M. and Nattinen K., *J. Organomet. Chem.*, **672**, 58 (2003).
4. Dötz K.H. and Jahr H.C., *Chem. Rec.*, **4**, 61 (2004).
5. Dötz K.H., Wenzel B. and Jahr H.C., *Top. Curr. Chem.*, **248**, 63 (2004).
6. Jahr H.C., Nieger M. and Dötz K.H., *Chem. Eur. J.*, **11**, 5333 (2005).
7. Künding E.P., Desobry V., Grivet C., Rudolph B. and Spichiger S., *Organometallics*, **6**, 1173 (1987).
8. Dötz K.H., Stinner C. and Nieger M., *J. Chem. Soc., Chem. Commun.*, 2535 (1995).

9. Oprunenko Y.F., Akhmedov N.G., Laikov D.N., Malyugina S.G., Mstislavsky V.I., Roznyatovsky V.A., Ustynyuk Y.A. and Ustynyuk N.A., *J. Organomet. Chem.*, **583**, 136 (1999).
10. Jahr H.C., Nieger M. and Dötz K.H., *Chem. Commun.*, 2866 (2003).
11. Pan J., Kampf J.W. and Ashe III A.J., *Organometallics*, **25**, 197 (2006).
12. Akhmedov N.G., Malyugina S.G., Mstislavsky V.I., Oprunenko Y.F., Roznyatovsky V.A., Batsanov A.S. and Ustynyuk N.A., *Organometallics*, **17**, 4607 (1998).
13. Merlic C.A., Walsh J.C., Tantillo D.J. and Houk K.N., *J. Am. Chem. Soc.*, **121**, 3596 (1999).
14. Oprunenko Y., Gloriosov I., Lyssenko K., Malyugina S., Mityuk D., Mstislavsky V., Günter H., von Firks G. and Ebener M., *J. Organomet. Chem.*, **656**, 27 (2002).
15. Dötz K.H., Stendel J., Jr., Müller S., Nieger M., Ketrat S. and Dolg M., *Organometallics*, **24**, 3219 (2005).
16. Stoddart M.W., Brownie J.H., Baird M.C. and Schmider H.L., *J. Organomet. Chem.*, **690**, 3440 (2005).
17. Pan J., Wang J., Banaszak Holl M.M., Kampf J.W. and Ashe III A.J., *Organometallics*, **25**, 3463 (2006).
18. Nambu M. and Siegel J.S., *J. Am. Chem. Soc.*, **110**, 3675 (1988).
19. Low A.A. and Hall M.B., *Int. J. Quantum Chem.*, **77**, 152 (2000).
20. Baldridge K.K. and Siegel J.S., *J. Phys. Chem.*, **100**, 6111 (1996).
21. Elass A., Mahieu J., Brocard J., Surpateanu G. and Vergoten G., *J. Mol. Struct. (Theochem)*, **475**, 261 (1999).
22. Arrais A., Diana E., Gervasio G., Gobetto R., Marabello D. and Stanghellini P.L., *Eur. J. Inorg. Chem.*, 1505 (2004).
23. Own Z.Y., Wang S.M., Chung J.F., Miller D.W. and Fu P.P., *Inorg. Chem.*, **32**, 152 (1993).
24. Güell M., Poater J., Luis J.M., Mó O., Yáñez M. and Solà M., *ChemPhysChem,* **6**, 2552 (2005).
25. Hubig S.M., Lindeman S.V. and Kochi J.K., *Coord. Chem. Rev.*, **200–202**, 831 (2006).
26. Merlic C.A., Zechman A.L. and Miller M.M., *J. Am. Chem. Soc.*, **123**, 11101 (2001).
27. Suresh C.H., Koga N. and Gadre S.R., *Organometallics*, **19**, 3008 (2000).
28. Mitchell R.H., Zhou P., Venugopalan S. and Dingle T.W., *J. Am. Chem. Soc.*, **112**, 7812 (1990).
29. Mitchell R.H., Chen Y., Khalifa N. and Zhou P., *J. Am. Chem. Soc.*, **120**, 1785 (1998).
30. Mitchell R.H., *Chem. Rev.*, **101**, 1301 (2001).
31. Mitchell R.H., Brkic Z., Berg D.J. and Barclay T.M., *J. Am. Chem. Soc.*, **124**, 11983 (2002).
32. Schleyer P.v.R., Kiran B., Simion D.V. and Sorensen T.S., *J. Am. Chem. Soc.*, **122**, 510 (2000).
33. Simion D.V. and Sorensen T.S., *J. Am. Chem. Soc.*, **118**, 7345 (1996).
34. Price J.T. and Sorensen T.S., *Can. J. Chem.*, **46**, 515 (1968).
35. Krygowski T.M., Cyrański M.K., Czarnocki Z., Häfelinger G. and Katritzky A.R., *Tetrahedron*, **56**, 1783 (2000).
36. Katritzky A.R., Jug K. and Oniciu D.C., *Chem. Rev.*, **101**, 1421 (2001).
37. Katritzky A.R., Barczynski P., Musumarra G., Pisano D. and Szafran M., *J. Am. Chem. Soc.*, **111**, 7 (1989).
38. Katritzky A.R., Karelson M., Sild S., Krygowski T.M. and Jug K., *J. Org. Chem.*, **63**, 5228 (1998).
39. Krygowski T.M. and Cyrański M.K., *Chem. Rev.*, **101**, 1385 (2001).
40. Cyrański M.K., Krygowski T.M., Katritzky A.R. and Schleyer P.v.R., *J. Org. Chem.*, **67**, 1333 (2002).
41. Kruszewski J. and Krygowski T.M., *Tetrahedron Lett.*, **13**, 3839 (1972).
42. Krygowski T.M., *J. Chem. Inf. Comp. Sci.*, **33**, 70 (1993).
43. Schleyer P.v.R., *Chem. Rev.*, **101**, 1115 (2001).
44. Schleyer P.v.R. and Jiao H., *Pure Appl. Chem.*, **68**, 209 (1996).
45. Schleyer P.v.R., Maerker C., Dransfeld A., Jiao H. and van Eikema Hommes N.J.R., *J. Am. Chem. Soc.*, **118**, 6317 (1996).
46. $NICS_{\pi}$ is the NICS obtained using only ring currents from π-electrons. Chen Z., Wannere C.S., Corminboeuf C., Puchta R. and Schleyer P.v.R., *Chem. Rev.*, **105**, 3842 (2005).
47. Poater J., Duran M., Solà M. and Silvi B., *Chem. Rev.*, **105**, 3911 (2005).
48. Poater J., Fradera X., Duran M. and Solà M., *Chem. Eur. J.*, **9**, 400 (2003).
49. Poater J., Fradera X., Duran M. and Solà M., *Chem. Eur. J.*, **9**, 1113 (2003).
50. Fradera X., Austen M.A. and Bader R.F.W., *J. Phys. Chem. A*, **103**, 304 (1999).
51. Fradera X., Poater J., Simon S., Duran M. and Solà M., *Theor. Chem. Acc.*, **108**, 214 (2002).
52. Bader R.F.W., Atoms in Molecules: A Quantum Theory. Clarendon, Oxford (1990).
53. Bader R.F.W., *Acc. Chem. Res.*, **18**, 9 (1985).

54. Bader R.F.W., *Chem. Rev.*, **91**, 893 (1991).
55. Portella G., Poater J., Bofill J.M., Alemany P. and Solà M., *J. Org. Chem.*, **70**, 2509 (2005); erratum, *ibid*, **70**, 4560 (2005).
56. Portella G., Poater J. and Solà M., *J. Phys. Org. Chem.*, **18**, 785 (2005).
57. Matito E., Duran M. and Solà M., *J. Chem. Phys.*, **122**, 014109 (2005); erratum, *ibid*, **125**, 059901 (2006).
58. Bultinck P., Ponec R. and Van Damme S., *J. Phys. Org. Chem.*, **18**, 706 (2005).
59. Bultinck P., Rafat M., Ponec R., van Gheluwe B., Carbó-Dorca R. and Popelier P.,*J. Phys. Chem. A*, **110**, 7642 (2006).
60. Frisch M.J., Trucks G.W., Schlegel H.B., Scuseria G.E., Robb M.A., Cheeseman J.R., Montgomery Jr. J.A., Vreven T., Kudin K.N., Burant J.C., Millam J.M., Iyengar S.S., Tomasi J., Barone V., Mennucci B., Cossi M., Scalmani G., Rega N., Petersson G.A., Nakatsuji H., Hada M., Ehara M., Toyota K., Fukuda R., Hasegawa J., Ishida M., Nakajima T., Honda Y., Kitao O., Nakai H., Klene M., Li X., Knox J.E., Hratchian H.P., Cross J.B., Bakken V., Adamo C., Jaramillo J., Gomperts R., Stratmann R.E., Yazyev O., Austin A.J., Cammi R., Pomelli C., Ochterski J.W., Ayala P.Y., Morokuma K., Voth G.A., Salvador P., Dannenberg J.J., Zakrzewski G., Dapprich S., Daniels A.D., Strain M.C., Farkas O., Malick D.K., Rabuck A.D., Raghavachari K., Foresman J.B., Ortiz J.V., Cui Q., Baboul A.G., Clifford S., Cioslowski J., Stefanov B.B., Liu G., Liashenko A., Piskorz P., Komaromi I., Martin R.L., Fox D.J., Keith T., Al-Laham M.A., Peng C.Y., Nanayakkara A., Challacombe M., Gill P.M.W., Johnson B., Chen W., Wong M.W., Gonzalez C. and Pople J.A., Gaussian 03, Revision C.01. Gaussian, Inc., Pittsburgh, PA (2003).
61. Biegler-König F.W., Bader R.F.W. and Tang T.-H., *J. Comput. Chem.*, **3**, 317 (1982).
62. Becke A.D., *J. Chem. Phys.*, **98**, 5648 (1993).
63. Lee C., Yang W. and Parr R.G., *Phys. Rev. B*, **37**, 785 (1988).
64. Stephens P.J., Devlin F.J., Chabalowski C.F. and Frisch M.J., *J. Phys. Chem.*, **98**, 11623 (1994).
65. Hehre W.J., Ditchfield R. and Pople J.A., *J. Chem. Phys.*, **56**, 2257 (1972).
66. Hariharan P.C. and Pople J.A., *Theor. Chim. Acta*, **28**, 213 (1973).
67. Francl M.M., Pietro W.J., Hehre W.J., Binkley J.S., Gordon M.S., Defrees D.J. and Pople J.A., *J. Chem. Phys*., **77**, 3654 (1982).
68. Wolinski K., Hilton J.F. and Pulay P., *J. Am. Chem. Soc.*, **112**, 8251 (1990).
69. Matito E., ESI-3D: Electron Sharing Indexes Program for 3D Molecular Space Partitioning. http://iqc.udg.es/~eduard/ESI. Girona, IQC (2006).
70. Poater J., Solà M., Duran M. and Fradera X., *Theor. Chem. Acc.*, **107**, 362 (2002).
71. Matito E., Solà M., Salvador P. and Duran M., *Faraday Discuss.*, **135**, 325 (2007).
72. Jeffrey G.A., Ruble J.R., McMullan R.K. and Pople J.A., *Proc. R. Soc. London A*, **414**, 47 (1987).
73. Christiansen O., Stanton J.F. and Gauss J., *J. Chem. Phys.*, **108**, 3987 (1998).
74. Bailey M.F. and Dahl L.F., *Inorg. Chem.*, **4**, 1314 (1965).
75. Rees B. and Coppens P., *Acta Cryst.*, **B29**, 2516 (1973).
76. Furet E. and Weber J., *Theor. Chim. Acta*, **91**, 157 (1995).
77. Mukerjee S.L., Lang R.F., Ju T., Kiss G., Hoff C.D. and Nolan S.P., *Inorg. Chem.*, **31**, 4885 (1992).
78. Albright T.A., Hofmann P., Hoffmann R., Lillya C.P. and Dobosh P.A.,*J. Am. Chem. Soc.*, **105**, 3396 (1983).
79. Cases M., Frenking G., Duran M. and Solà M., *Organometallics*, **21**, 4182 (2002).
80. Cioslowski J., *J. Am. Chem. Soc.*, **111**, 8333 (1989).
81. Cyrański M.K. and Krygowski T.M., *Tetrahedron*, **55**, 6205 (1999).
82. Feixas F., Matito E., Poater J. and Solà M., *J. Phys. Chem. A*., submitted for publication (2007).
83. Corminboeuf C., Heine T., Seifert G., Schleyer P.v.R. and Weber J., *Phys. Chem. Chem. Phys.*, **6**, 273 (2004).
84. Fallah-Bagher-Shaidaei H., Wannere C.S., Corminboeuf C., Puchta R. and Schleyer P.v.R., *Org. Lett.*, **8**, 863 (2006).
85. Poater J., Bofill J.M., Alemany P. and Solà M., *J. Org. Chem.*, **71**, 1700 (2006).
86. Osuna S., Poater J., Bofill J.M., Alemany P. and Solà M., *Chem. Phys. Lett.*, **428**, 191 (2006).